

# CrystEngComm

Accepted Manuscript



This is an *Accepted Manuscript*, which has been through the Royal Society of Chemistry peer review process and has been accepted for publication.

*Accepted Manuscripts* are published online shortly after acceptance, before technical editing, formatting and proof reading. Using this free service, authors can make their results available to the community, in citable form, before we publish the edited article. We will replace this *Accepted Manuscript* with the edited and formatted *Advance Article* as soon as it is available.

You can find more information about *Accepted Manuscripts* in the [Information for Authors](#).

Please note that technical editing may introduce minor changes to the text and/or graphics, which may alter content. The journal's standard [Terms & Conditions](#) and the [Ethical guidelines](#) still apply. In no event shall the Royal Society of Chemistry be held responsible for any errors or omissions in this *Accepted Manuscript* or any consequences arising from the use of any information it contains.

## ARTICLE

Cite this: DOI: 10.1039/x0xx00000x

# Hydrogen bonded-extended lanthanide coordination polymers decorated with 2,3-thiophenedicarboxylate and oxalate: synthesis, structures, and properties

Received 00th January 2014,  
Accepted 00th January 2014

DOI: 10.1039/x0xx00000x

www.rsc.org/

Zhao-Hao Li,<sup>a</sup> Li-Ping Xue<sup>\*a</sup>, Li-Li Shan<sup>a</sup>, Bang-Tun Zhao<sup>\*a</sup>, Jian Kan<sup>b</sup> and Wei-Ping Su<sup>b</sup>

Five new lanthanide coordination polymers,  $\{[\text{Ln}_2(\text{tdc})_2(\text{C}_2\text{O}_4)(\text{H}_2\text{O})_4]\cdot(\text{H}_2\text{O})\}_n$  (Ln = Nd (**1**), Eu (**2**), Gd (**3**), Tb (**4**), Ho (**5**); H<sub>2</sub>tdc = 2,3-thiophenedicarboxylic acid), have been synthesized by hydrothermal reactions of H<sub>2</sub>tdc, sodium oxalate and corresponding lanthanide nitrate. Crystallographic data show that **1–5** are isomorphous and crystallize in the monoclinic space group C2/c. Each complex contains an oxalate-linked two-dimensional (2D) **sql** layer structure based on dinuclear  $[\text{Ln}_2(\text{tdc})_2(\text{H}_2\text{O})_4]$  building units. Then the 2D layers are further extended by intermolecule hydrogen bonds to form a three-dimensional (3D) supramolecular network with **sxb** topology. Compounds **2** and **4** display luminescence emission in the visible region, while compounds **1** and **5** exhibit luminescence emission in the near IR region. Dehydrated **1** as a Lewis acid catalyst exhibits high catalytic activity and stability in acetalization reaction under mild conditions. Furthermore, infrared, thermogravimetric analysis, elemental analyses, and powder X-ray diffraction properties of these compounds are also studied.

## Introduction

Due to fundamental studies and possible applications, the construction of lanthanide-based coordination polymers (LnCPs) with higher dimensional structures is rapidly growing.<sup>1</sup> Lanthanide ions are normally used as connectors in the construction of new CPs, not only for its foreseen and controllable mode of coordination, but also for its chemical characteristics such as luminescence, magnetism, and hard Lewis acidity.<sup>2</sup> To date, many LnCPs with various structures and properties have been obtained. According to literature, widely used ligands to construct LnCPs are polycarboxylic acids, owing to their rich coordination modes and high affinity of Ln<sup>3+</sup> ions for the oxygen atom. Among them, benzenepolycarboxylic acid,<sup>3</sup> pyridinecarboxylic acid,<sup>4</sup> and imidazolecarboxylic acid<sup>5</sup> have been widely employed to build LnCPs. Noted that small auxiliary anions play an important role in regulating LnCPs. In this regard, anions, such as oxalate, acetate, halides and sulfate have been well employed to synthesize LnCPs.<sup>6</sup> These anions have versatile coordination modes which could help to satisfy high coordination numbers of Ln<sup>3+</sup> ions and while might exert a synergistic influence in the structural control.

Lately, LnCPs decorated by thiophenedicarboxylic acids have received increasing attention due to their improved

luminescence intensity and interesting topologies.<sup>7</sup> However, most of the work has been devoted in synthesizing and characterization of LnCPs built from available 2,5-thiophenedicarboxylic acid.<sup>7a-7i</sup> 3,4-thiophenedicarboxylic acid is currently being used as a linker in our group and three isostructural LnCPs with an interesting reversible de- and rehydration behavior were obtained.<sup>7j</sup> Considering structural similarity, isomeric 2,3-thiophenedicarboxylic acid (H<sub>2</sub>tdc) may be a good candidate to produce LnCPs.<sup>8</sup>

Here, we chose H<sub>2</sub>tdc/oxalate/water system to build LnCPs, based on the following considerations: (1) H<sub>2</sub>tdc, as a multidentate ligand with two neighboring carboxylate groups, may show various coordination modes, which makes it a useful bridge to prepare LnCPs; (2) oxalate, as an old but evergreen bis-bidentate connectors, can facilitate to tune extended structures by bridging Ln<sup>3+</sup> ions; (3) water, as an economic and green solvent, may participate in coordinating and satisfying the coordination geometry of Ln<sup>3+</sup> ions while uncoordinated water can induce different structure of LnCPs in the crystal engineering. Moreover, coordinated and uncoordinated water may be removed easily to generate coordinatively unsaturated Ln<sup>3+</sup> ions connecting points as potential Lewis acid sites.

To this end, we are inspired to explore and synthesize new LnCPs with mixed ligands and different Ln<sup>3+</sup> ions. In this contribution, five hydrogen bonded-extended three-dimensional

(3D) supramolecular LnCPs decorated by H<sub>2</sub>tdc and oxalate mixed ligands, {[Ln<sub>2</sub>(tdc)<sub>2</sub>(C<sub>2</sub>O<sub>4</sub>)(H<sub>2</sub>O)<sub>4</sub>·(H<sub>2</sub>O)]<sub>n</sub> (Ln = Nd(**1**), Eu (**2**), Gd (**3**), Tb (**4**), Ho (**5**)) were hydrothermally synthesized. Their spectral, thermal, photoluminescence and catalytic properties are described.

## Experimental section

### Materials and methods

The ligand 2,3-thiophenedicarboxylic acid was prepared according to a literature procedure.<sup>9</sup> Other reagents were purchased commercially and used without further purification. The solvothermal reaction was performed in a 25 mL Teflon-lined stainless steel autoclave under autogenous pressure. The IR spectra were recorded on a Nicolet Avatar-360 spectrometer in the range of 4000 to 400 cm<sup>-1</sup>. Elemental analyses for C, H, and N were carried out on a Flash 2000 elemental analyzer. Powder X-ray diffraction (PXRD) measurements were performed on a Bruker D8-ADVANCE X-ray diffractometer with Cu K $\alpha$  radiation ( $\lambda = 1.5418 \text{ \AA}$ ). Thermogravimetric analyses were carried out on a SDT Q600 thermogravimetric analyzer. A platinum pan was used for heating the sample with a heating rate of 10 °C/min under a N<sub>2</sub> atmosphere. Luminescent spectra were recorded with a Hitachi F4500 fluorescence spectrophotometer. <sup>1</sup>H NMR spectra was measured with a Bruker AVANCE-400 NMR spectrometer.

**Syntheses of compounds** {[Ln<sub>2</sub>(tdc)<sub>2</sub>(C<sub>2</sub>O<sub>4</sub>)(H<sub>2</sub>O)<sub>4</sub>·(H<sub>2</sub>O)]<sub>n</sub> (Ln = Nd(**1**), Eu(**2**), Gd(**3**), Tb(**4**), Ho(**5**))

The same procedure was employed in preparing all lanthanide complexes. A mixture of H<sub>2</sub>tdc (0.25 mmol, 0.0430 g), Ln(NO<sub>3</sub>)<sub>3</sub>·6H<sub>2</sub>O (0.25 mmol, (**1**) = Nd(NO<sub>3</sub>)<sub>3</sub>·6H<sub>2</sub>O, 0.1096 g, (**2**) = Eu(NO<sub>3</sub>)<sub>3</sub>·6H<sub>2</sub>O, 0.1115 g, (**3**) = Gd(NO<sub>3</sub>)<sub>3</sub>·6H<sub>2</sub>O, 0.1128 g, (**4**) = Tb(NO<sub>3</sub>)<sub>3</sub>·5H<sub>2</sub>O, 0.1133 g, (**5**) = Ho(NO<sub>3</sub>)<sub>3</sub>·5H<sub>2</sub>O, 0.1147 g), Na<sub>2</sub>C<sub>2</sub>O<sub>4</sub> (0.25 mmol, 0.0335 g), and deionized water (8.0 mL) was sealed in a 25 mL Teflon-lined stainless steel vessel and heated at 140 °C for 5 days under autogenous pressure, followed by cooling to room temperature at a rate of 5 °C h<sup>-1</sup>. Block single crystals were collected. For **1**, yield: 53.8% (based on neodymium). Elemental analysis calcd (%) for C<sub>14</sub>H<sub>14</sub>O<sub>17</sub>S<sub>2</sub>Nd<sub>2</sub>: C, 19.80; H, 1.65. Found: C, 19.82; H, 1.67. IR (v/cm<sup>-1</sup>): 3234 (br), 3125 (w), 1661 (m), 1541 (m), 1506 (s), 1422 (m), 1387 (m), 1341 (w), 1311 (m), 1243 (w), 1193 (w), 1124 (w), 1110 (m), 1063 (m), 1013 (m), 972 (w), 930 (m), 838 (s), 796 (s), 751 (s). For **2**, yield: 35.8%. Elemental analysis calcd (%) for C<sub>14</sub>H<sub>14</sub>O<sub>17</sub>S<sub>2</sub>Eu<sub>2</sub>: C, 25.52; H, 1.42. Found: C, 25.49; H, 1.46. IR (v/cm<sup>-1</sup>): 3234 (br), 3125 (w), 1661 (m), 1541 (m), 1506 (s), 1422 (m), 1387 (m), 1341 (w), 1311 (m), 1243 (w), 1193 (w), 1124 (w), 1110 (m), 1063 (m), 1013 (m), 972 (w), 930 (m), 838 (s), 796 (s), 751 (s). For **3**, yield: 35.8%. Elemental analysis calcd (%) for C<sub>14</sub>H<sub>14</sub>O<sub>17</sub>S<sub>2</sub>Gd<sub>2</sub>: C, 25.52; H, 1.42. Found: C, 25.49; H, 1.46. IR (v/cm<sup>-1</sup>): 3229 (br), 3117 (w), 1664 (m), 1539 (w), 1506 (m), 1432 (s), 1388 (s), 1346 (w), 1314 (m), 1195 (m), 1125 (m), 1083 (w), 973 (m), 860 (m), 840 (m), 798 (s), 761 (m), 761 (m), 688 (w), 669 (m). For **4**, yield: 35.8%. Elemental analysis

calcd (%) for C<sub>14</sub>H<sub>14</sub>O<sub>17</sub>S<sub>2</sub>Tb<sub>2</sub>: C, 25.52; H, 1.42. Found: C, 25.49; H, 1.46. IR (v/cm<sup>-1</sup>): 3229 (br), 3117 (w), 1664 (m), 1539 (w), 1506 (m), 1432 (s), 1388 (s), 1346 (w), 1314 (m), 1195 (m), 1125 (m), 1083 (w), 973 (m), 860 (m), 840 (m), 798 (s), 761 (m), 761 (m), 688 (w), 669 (m). For **5**, yield: 36.2%. Elemental analysis calcd (%) for C<sub>14</sub>H<sub>14</sub>O<sub>17</sub>S<sub>2</sub>Ho<sub>2</sub>: C, 25.52; H, 1.42. Found: C, 25.49; H, 1.46. IR (v/cm<sup>-1</sup>): 3229 (br), 3117 (w), 1664 (m), 1539 (w), 1506 (m), 1432 (s), 1388 (s), 1346 (w), 1314 (m), 1195 (m), 1125 (m), 1083 (w), 973 (m), 860 (m), 840 (m), 798 (s), 761 (m), 761 (m), 688 (w), 669 (m).

### X-ray crystallography

The crystal structure data of **1–5** were collected on Bruker SMART APEX II CCD diffractometer equipped with a graphite-monochromated Mo K $\alpha$  ( $\lambda = 0.71073 \text{ \AA}$ ) radiation using an  $\omega$  scan mode at 293 K. An empirical absorption correction was applied using the SADABS program.<sup>10</sup> The structures were solved by direct methods and refined by full-matrix least-squares on  $F^2$  using the SHELXL-97 program package.<sup>11</sup> All non-hydrogen atoms were refined with anisotropic displacement parameters. The hydrogen atoms on water molecules were located from difference Fourier maps and were refined using a riding model. Other hydrogen atoms were placed at the calculation positions. A summary of the crystallographic data and the selected bond lengths of **1–5** is listed in Table S1 of ESI and Table S2 of ESI. Hydrogen bond parameters of **1** are listed in Table S3 of ESI, respectively.

### Catalytic Study

The acetalization reaction of aldehyde was carried out at room temperature. Into a Pyrex-glass screw cap vial, dehydrated **1** (5 mol %) and benzaldehyde (1 mmol) were successively placed in 10 ml dry methanol under a nitrogen atmosphere. Then the reaction mixture was stirred for 12 h. After the reaction was completed, the solid catalyst was separated by centrifuge and the crude product was purified by column chromatography. The resulted product was dried under vacuum, weighted and characterized by <sup>1</sup>H NMR spectroscopy. In the consecutive recycling experiment, recovered catalyst **1** was washed with acetone to remove adsorbed organic substrate, followed by activated at 200 °C for 2 h prior to being used.

## Results and discussions

### Synthesis and structure description

As well known, high temperature and pressure during the course of hydrothermal reactions can dramatically enhance the ligand solubility and the reactivity of reactants. Then, single crystals of **1–5** were obtained in the same conditions by the hydrothermal reactions of lanthanide nitrates with 2,3-thiophenedicarboxylic acid and oxalate in water at 140 °C. It is noted that the same LnCPs were also obtained in the absence of oxalate ligands but at higher 160 °C in lower yields. The oxalate ligand could be in situ obtained from the reaction at higher temperature and the generation mechanism should be

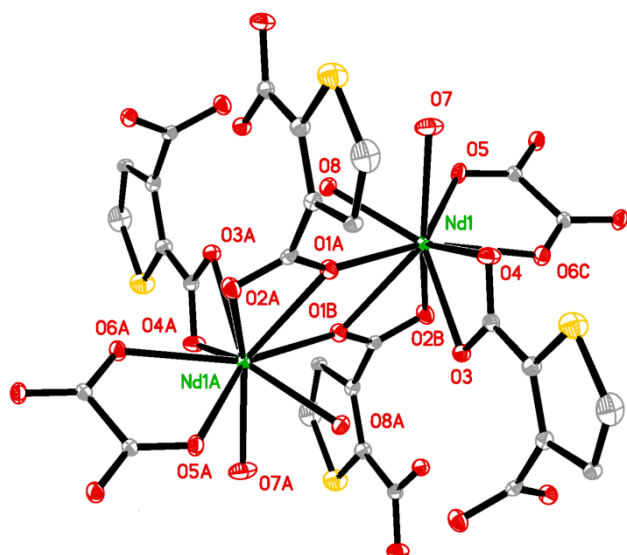


**Fig. 1** Coordination environment of  $\text{Nd}^{3+}$  ions and corresponding a  $\text{Nd}_2\text{O}_2$  subunit in **1**. All hydrogen atoms are omitted for clarity. Symmetry transformation used to generate equivalent atoms: (A)  $x, 1 + y, z$ ; (B)  $0.5 - x, 1.5 - y, 1 - z$ ; (C)  $-x, 2 - y, 1 - z$ .

similar to other reported decarboxylation of aromatic carboxylic acids.<sup>12</sup> Compounds **1–5** are air-stable and insoluble in water and common organic solvents, such as acetone, chloroform, toluene, acetonitrile, methanol, and ethanol.

Single-crystal X-ray analysis of **1–5** indicates that they are isomorphous and crystallize in monoclinic space group  $C2/c$ . Thus, only the crystal structure of **1** will be described herein as a representative example. In the asymmetrical unit, there is one unique  $\text{Nd}^{3+}$  ion, one crystallographically independent  $\text{tdc}^{2-}$  anion, one half oxalate anion, two coordinated water molecules, as well as half a crystalline water molecule lying on the binary axis (Fig. 1). The central  $\text{Nd}^{3+}$  ion is nine coordinated with distorted tricapped trigonal prism geometries: five carboxylate

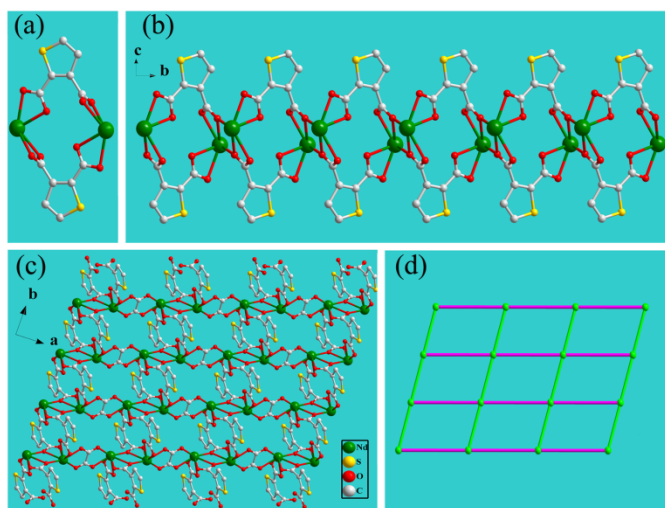


**Fig. 2** (a) The SUB structure of  $[\text{Nd}_2(\text{tdc})_2(\text{H}_2\text{O})_4]$ . (b) View of the 1D chain with  $\text{Nd}_2\text{O}_2$  subunits. (c) View of the 2D structure of **1**. (d) Schematic representation of the 4-connected sql sheet of **1**. All hydrogen atoms and water molecules are omitted for clarity.

oxygen from three  $\text{tdc}^{2-}$  anions, two oxygen from one oxalate anion, together with two coordinated water molecules. The  $\text{Nd}-\text{O}$  bond lengths range from 2.443(2) to 2.631(2) Å, which are expected as those observed in reported  $\text{Nd}^{3+}$  compounds.<sup>6a</sup> The bond angles of  $\text{O}-\text{Nd}-\text{O}$  are in the range of 50.29(7)° to 148.96(9)°. Owing to the effect of lanthanide contraction, the average bond length of  $\text{Ln}-\text{O}$ , which decreases with the decreasing radii of lanthanide ions. The average distances of  $\text{Ln}-\text{O}$  for **1**, **2**, **3**, **4** and **5** are 2.507(3), 2.446(3), 2.458(3), 2.446(4), and 2.422(3) Å, respectively. The  $\text{tdc}^{2-}$  anion takes a  $(\kappa^2-\kappa^1-\mu_2)-(\kappa^2)-\mu_3$  coordination mode (ESI, Scheme 1) bridging three  $\text{Nd}^{3+}$  ions, while the oxalate group shows a bis-bidentate coordination mode linking two  $\text{Nd}^{3+}$  ions. Two  $\text{Nd}^{3+}$  ions are linked by two  $\text{tdc}^{2-}$  anions, forming a centrosymmetric dinuclear secondary building unit (SBU) of  $[\text{Nd}_2(\text{tdc})_2(\text{H}_2\text{O})_4]$  with a  $\text{Nd}\cdots\text{Nd}$  distance of 6.7516(8) Å (Fig. 2a). These SBUs are connected to each other along the  $b$  axis through double chelating/bridging carboxylate oxygen atoms, resulting in a one-dimensional (1D) chain containing a  $\text{Nd}_2\text{O}_2$  subunit with an edge-sharing polyhedron along  $b$  axis (Fig. 2b). The  $\text{Nd}\cdots\text{Nd}$  distance and  $\text{O}-\text{Nd}-\text{O}$  angle within the  $\text{Nd}_2\text{O}_2$  subunits are 4.2979(7) Å and 114.843(111)°, respectively. Adjacent chains are alternatively connected by oxalate anions into a two-dimensional (2D) layer, exhibiting a ladder-like network with the chains as sharing sidepieces and the oxalate ligands as rungs (Fig. 2c). The nearest distance of  $\text{Nd}\cdots\text{Nd}$  between chains is 6.4171(8) Å. From a topological viewpoint, central  $\text{Nd}_2\text{O}_2$  subunits could be considered as four-connected nodes and

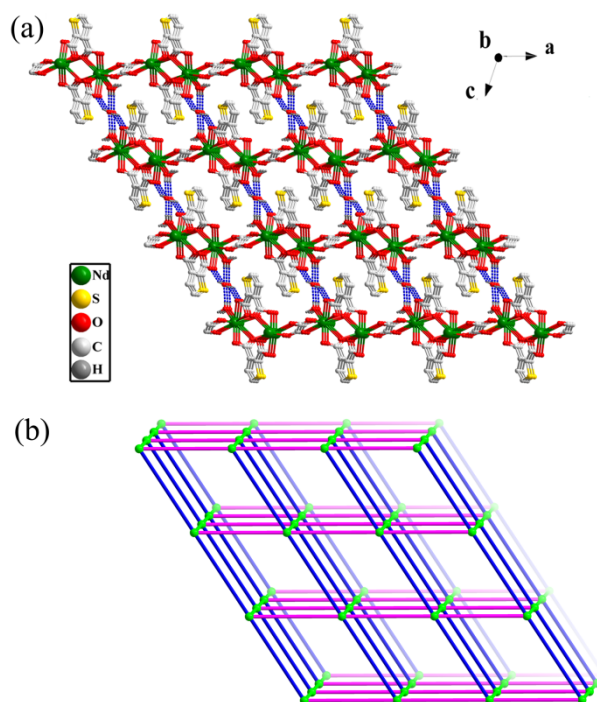


**Fig. 3** (a) 3D supramolecular structure constructed from intermolecular hydrogen bonds in **1**. (b) Schematic representation of the 6-connected sxb topology. Blue bonds represent intermolecular hydrogen bonding bridges.

tdc<sup>2-</sup> anions as linear linkers, the 2D layer can be simplified to a 4-connected **sql** sheet with {4<sup>4</sup>.6<sup>2</sup>} topology (Fig. 2d).

It is worthy to note that there exist two strong intermolecular hydrogen bonding interactions and O...O distances are 2.746(3), 2.756(3) Å, respectively. Thus, the adjacent alternative layers are held together along the *c* axis by the intermolecular hydrogen bonds, generating a 3D supramolecular network with unusual 6-connected **sbx** topology (Schäfli symbol 4<sup>8</sup>5<sup>4</sup>6<sup>3</sup>), in which the lattice water molecules act as linkers (Fig. 3).<sup>13</sup> In addition, there is significant offset C–H... $\pi$  stacking interactions ( $d_{\text{H-centroid}} = 2.810$  Å) and extensive intramolecular O–H...O hydrogen bonding interactions between the coordinated water and carboxyl oxygen atoms (ESI, Fig. S1†). Undoubtedly, hydrogen bonds and C–H... $\pi$  interactions give rise to a reinforcement of the stabilization of the 3D supramolecular architecture.

### Spectral and thermal characterizations

The powder X-ray diffraction (PXRD) patterns of **1–5** are revealed with the pattern simulated on the basis of single crystal structures (ESI, Fig. S2†). The positions of the diffraction peaks in both patterns correspond well, indicating high crystalline phase purity and isostructural structure of the synthesized **1–5**. The IR spectra of **1–5** are similar and the broad absorption band around 3200 cm<sup>-1</sup> may be assigned to the characteristic peaks of OH stretching vibrations from water molecules. The strong vibrations appearing around 1600 and 1400 cm<sup>-1</sup> correspond to the asymmetric and symmetric stretching vibrations of the carboxylate group, respectively. The absence of strong absorption bands ranging from 1690 to 1730 cm<sup>-1</sup> indicates H<sub>2</sub>tdc and oxalate ligands are deprotonated. The IR spectra of **1–5** are in accordance with the results of the X-ray diffraction analysis.

To study the thermal stabilities of **1–5**, TGA in N<sub>2</sub> atmosphere with a heating rate of 10 °C /min were performed on polycrystalline samples to determine their thermal stabilities from 30 to 800 °C (ESI, Fig. S3†). Since **1–5** show almost the same thermal decomposition process, **1** is selected as a representative example to illustrate them in detail. The TGA curve of **1** indicates that there is no mass change from room temperature to 173 °C on the whole, and the weight loss of 11.26% from 173 °C to 240 °C can be ascribed to the removal of one lattice water and four coordinated water molecules (calcd = 11.16%). No further weight loss is observed between 240 and 350 °C, indicating during this temperature range, the crystallinity of the dehydrated product remains unchanged. Above 350 °C, the observed weight loss corresponds to the decomposition of the organic ligands and the collapse of the whole framework. The remaining weight loss corresponds to the formation of Nd<sub>2</sub>O<sub>3</sub> (calcd. 41.6%).

### Luminescent Properties

LnCPs have excellent luminescent properties due to internal 4f–4f transitions. Hence, the solid-state luminescent behaviors are measured at room temperature (Fig. 4). **2** emits intense red light upon excitation at 380 nm and the emission peaks at 581, 594,

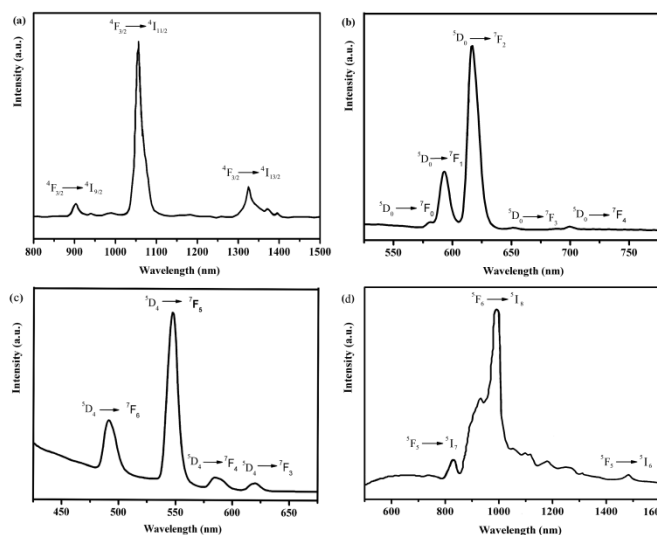


**Fig. 4** Solid-state emission spectra of (a) **1**, (b) **2**, (c) **3**, and (d) **5** at room temperature upon excitation at 330, 380, 370 and 340 nm, respectively.

618, 650, 698 nm in the visible region correspond to the characteristic transitions from <sup>5</sup>D<sub>0</sub> → <sup>7</sup>F<sub>J</sub> (J = 0, 1, 2, 3, and 4) of Eu<sup>3+</sup> ion. According to Judd-Ofelt theory, the electric dipole transition <sup>5</sup>D<sub>0</sub> → <sup>7</sup>F<sub>2</sub> is hypersensitive to the coordination environment of the Eu<sup>3+</sup> ion, which is only permitted on the condition when the Eu<sup>3+</sup> ion possess a site without an inversion center.<sup>14</sup> Moreover, the emission peak at 618 nm is composed of a single intense peak and responsible for the intense red emission. The symmetry-forbidden weak emission peak <sup>5</sup>D<sub>0</sub> → <sup>7</sup>F<sub>0</sub> at 581 nm indicates that the Eu<sup>3+</sup> ions occupy a low symmetry site. The emission peak <sup>5</sup>D<sub>0</sub> → <sup>7</sup>F<sub>1</sub> at 594 nm is a magnetic dipole transition, and its intensity is almost independent upon the crystal field change acting on the Eu<sup>3+</sup> ions. **4** emits green light under excitation of 340 nm and displays a typical emission peaks <sup>5</sup>D<sub>4</sub> → <sup>7</sup>F<sub>J</sub> (J = 6, 5, 4, 3) at 487, 545, 585, and 620 nm, in which the strongest emission corresponds to <sup>5</sup>D<sub>4</sub> → <sup>7</sup>F<sub>5</sub> transition of Tb<sup>3+</sup> ions. Noted that no other emission bands based on H<sub>2</sub>tdc ligand are observed, indicating that the ligands transfer the excitation energy to the Eu<sup>3+</sup> and Tb<sup>3+</sup> ions. The luminescent investigations on **2** and **4** suggest that H<sub>2</sub>tdc ligand may sensitize the luminescence of Eu<sup>3+</sup> and Tb<sup>3+</sup> ions. Considering that good thermal stabilities, **2** and **4** could find application as potential light-emitting candidates.

**1** and **5** show emission in the infrared part of the emission spectrum. The typical emission of **1** around 897, 1067 and 1335 nm are tentatively assigned to be <sup>4</sup>F<sub>3/2</sub> → <sup>4</sup>I<sub>9/2</sub>, <sup>4</sup>F<sub>3/2</sub> → <sup>4</sup>I<sub>9/2</sub> and <sup>4</sup>F<sub>3/2</sub> → <sup>4</sup>I<sub>9/2</sub> transitions, respectively, where the peak at 1067 nm is the strongest. For **5**, the NIR emission spectrum consists of three bands at 989, 1177 and 1478 nm, which are attributed to <sup>5</sup>F<sub>5</sub> → <sup>5</sup>I<sub>7</sub>, <sup>5</sup>I<sub>6</sub> → <sup>5</sup>I<sub>8</sub> and <sup>5</sup>F<sub>5</sub> → <sup>5</sup>I<sub>6</sub> transitions, respectively.

### Catalytic Test

As is well-known, organic transformations catalyzed by Ln<sup>3+</sup> ions can be achieved due to Lewis acid strength of Ln<sup>3+</sup> ions. In **1–5**, auxiliary oxalate ligand and coordinated water as

coordination blocking molecules, allow the CPs dimensionality control and this type of dehydrated material has coordinatively unsaturated  $\text{Ln}^{3+}$  Lewis acid sites and may exhibit higher catalytic activity. Here, dehydrated **1** as typical catalysts were examined in the acetalization reaction of benzaldehyde with methanol.

The sample of **1** was activated at 200 °C for 2 h before the catalytic test. When the reaction was performed under mild conditions (room temperature, 5 mol % catalyst, 12 h), resulting in (dimethoxymethyl)benzene as the only product in a 82% isolated yield. For comparison, neodymium nitrate hexahydrate was used as a catalyst for this reaction. However, there was no formation of (dimethoxymethyl)benzene under identical conditions, indicating that the activity of neodymium nitrate hexahydrate directly as a Lewis acid in the system is diminished. Moreover, the acetalization reaction did not proceed under identical conditions devoid of dehydrated **1** catalyst, which indicate dehydrated **1** has the ability to acts as an efficient Lewis acid catalyst for the acetalization reaction. For practical application, the lifetime of the catalysts and their reusability are very important factors. Dehydrated **1** could be isolated from the reaction suspension by filtration, washed and dried at 200 °C for 2 h again. Recycled **1** was then used under the same reaction conditions giving 80%, 81%, and 84% isolated yield for the second, third and fourth runs, respectively (Fig. 5). This demonstrates the dehydrated **1** is a reusable catalyst and could be reused at least three runs without any loss of activity. The stability of dehydrated **1** catalyst was directly confirmed by the similar PXRD pattern of fresh dehydrated **1** and sample after run 4 (ESI, Fig. S4†). A plausible mechanism of the reaction is that unsaturated  $\text{Nd}^{3+}$  ions located at the surfaces act as a Lewis acid active sites after  $\text{H}_2\text{O}$  molecules are removed.

Note that, the acetalization reaction was also carried out with other dehydrated catalysts. The experimental results revealed dehydrated **2**, **3**, and **4** exhibited moderate activity with 53%,

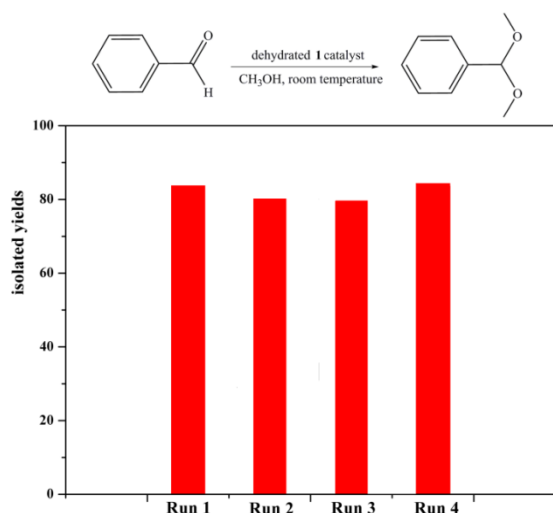


**Fig. 5** Four consecutive recycling runs of the acetalization reaction catalyzed by dehydrated **1**.

45 and 40% yields, respectively, while **5** afforded a lower yield (19%) even after extended reaction time (24 h). It is well known that relative Lewis acidities of  $\text{Ln}^{3+}$  ions increase in the order:  $\text{Nd} > \text{Eu} > \text{Gd} > \text{Tb} > \text{Ho}$ . The catalytic activity of this type of dehydrated catalysts decreased with the reduction of  $\text{Ln}^{3+}$  ionic radius, which may be owing to the increased steric hindrance between reactive substrates and coordinatively unsaturated  $\text{Ln}^{3+}$  ions in the solid-state LnCPs.<sup>15</sup>

## Conclusions

In summary, we have successfully constructed five new coordination polymers by reacting 2,3-thiophenedicarboxylic acid with lanthanide ions under hydrothermal conditions. All compounds represent 2D **sql** networks and further interlink into 3D supramolecular networks with **sxb** topology. Thermal behaviours indicate them to be stable, in combination with the strong emissions properties of lanthanide compounds make **2** and **4** eminently suitable for potential application as red and green luminescent materials. Furthermore, dehydrated **1** as a Lewis acid catalyst exhibits high catalytic activity in acetalization reaction under mild conditions

## Acknowledgements

This work was supported by the Natural Science Foundation of China (21401097), the Program for Innovative Research Team (in Science and Technology) in University of Henan Province (14IRTSTHN008) and the Natural Science Foundation of Henan Province (132300410326) for the financial support.

## Notes and references

<sup>a</sup> College of Chemistry and Chemical Engineering, Luoyang Normal University, Luoyang, Henan 471022, P. R. China, E-mail: lpxue@163.com.

<sup>b</sup> State Key Laboratory of Structural Chemistry, Fujian Institute of Research on the Structure of Matter, The Chinese Academy of Sciences, Fuzhou, Fujian 350002, P. R. China.

† Electronic Supplementary Information (ESI) available: crystal data for **1–5**, selected bond lengths, hydrogen bond parameters, coordination modes of 2,3-thiophenedicarboxylate and oxalate, PXRD, as well as TG analysis and <sup>1</sup>H NMR spectroscopy. CCDC 1020432 (**1**), 1020433 (**2**), 1020434 (**3**), 1020435 (**4**), 1020436 (**5**). For ESI and crystallographic data in CIF or other electronic format, See DOI: 10.1039/b000000x/

- (a) J.-P. Zhang, Y.-B. Zhang, J.-B. Lin and X.-M. Chen, *Chem. Rev.*, 2012, **112**, 1001; (b) J.-R. Li, R. J. Kuppler and H.-C. Zhou, *Chem. Soc. Rev.*, 2009, **38**, 1477; (c) L. Ma, C. Abney and W. Lin, *Chem. Soc. Rev.*, 2009, **38**, 1248.
- (a) J. C. G. Bünzli and C. Piguet, *Chem. Soc. Rev.*, 2005, **34**, 1048. (b) A. H. Morrish, *The Physical Principles of Magnetism*; Wiley: New York, 1965; (c) A. Corma and H. García, *Chem. Rev.*, 2003, **103**, 4307; (d) Y.-N. Gong, L. Jiang and T.-B. Lu, *Chem. Commun.*, 2013, **49**, 11113.

- 3 (a) H. He, H. Ma, D. Sun, L. Zhang, R. Wang and D. Sun, *Cryst. Growth Des.*, 2013, **13**, 3154; (b) Y. Wan, L. Zhang, L. Jin, S. Gao and S. Lu, *Inorg. Chem.*, 2003, **42**, 4985; (c) T. M. Reineke, M. Eddaoudi, M. O'Keeffe and O. M. Yaghi, *Angew. Chem. Int. Ed.*, 1999, **38**, 2590.
- 4 (a) B. Zhao, L. Yi, Y. Dai, X.-Y. Chen, P. Cheng, D.-Z. Liao, S.-P. Yan and Z.-H. Jiang, *Inorg. Chem.*, 2005, **44**, 911; (b) C. Qin, X. L. Wang, E. B. Wang and Z. M. Su, *Inorg. Chem.*, 2005, **44**, 7122; (c) B. Chen, L. Wang, Y. Xiao, F. R. Fronczek, M. Xue, Y. Cui and G. Qian, *Angew. Chem. Int. Ed.*, 2009, **48**, 500; (d) P. Mahata, K. V. Ramya and S. Natarajan, *Chem.-Eur. J.*, 2008, **14**, 5839; (e) J. Xu, W. Su and M. Hong, *Cryst. Growth Des.*, 2011, **11**, 337.
- 5 (a) W.-G. Lu, L. Jiang and T.-B. Lu, *Cryst. Growth Des.*, 2010, **10**, 4310; (b) Y.-Q. Sun, J. Zhang, Y.-M. Chen and G.-Y. Yang, *Angew. Chem. Int. Ed.*, 2005, **44**, 2814; (c) T. K. Maji, G. Mostafa, H.-C. Chang and S. Kitagawa, *Chem. Commun.*, 2005, 2436; (d) X. Feng, J. Wang, B. Liu, L. Wang, J. Zhao and S. Ng, *Cryst. Growth Des.*, 2012, **12**, 927.
- 6 (a) J. Xu, J. Cheng, W. Su and M. Hong, *Cryst. Growth Des.*, 2011, **11**, 2294; (b) M.-S. Liu, Q.-Y. Yu, Y.-P. Cai, C.-Y. Su, X.-M. Lin, X.-X. Zhou and J.-W. Cai, *Cryst. Growth Des.*, 2008, **8**, 4083; (c) Z.-H. Li, L.-P. Xue, B.-T. Zhao, J. Kan and W.-P. Su, *CrystEngComm*, 2012, **14**, 8485; (d) R. Feng, L. Chen, Q.-H. Chen, X.-C. Shan, Y.-L. Gai, F.-L. Jiang, and M.-C. Hong, *Cryst. Growth Des.*, 2011, **11**, 1705; (e) B. Tan, Z.-L. Xie, M.-L. Feng, B. Hu, Z.-F. Wu and X.-Y. Huang, *Dalton Trans.*, 2012, **41**, 10576; (f) C. J. Höller and K. Müller-Buschbaum, *Inorg. Chem.*, 2008, **47**, 10141; (g) Z.-X. Wang, Q.-F. Wu, H.-J. Liu, M. Shao, H.-P. Xiao and M.-X. Li, *CrystEngComm*, 2010, **12**, 1139; (h) R. F. D'Vries, M. Iglesias, N. Snejko, S. Alvarez-Garcia, E. Gutiérrez-Puebla and M. A. Monge, *J. Mater. Chem.*, 2012, **22**, 1191.
- 7 (a) J.-G. Wang, C.-C. Huang, X.-H. Huang and D.-S. Liu, *Cryst. Growth Des.*, 2008, **8**, 795; (b) L. F. Marques, M. V. dos Santos, S. J.L. Ribeiro, E. Ernesto Castellano and F. C. Machado, *Polyhedron*, 2012, **38**, 149; (c) Z. Chen, B. Zhao, P. Cheng, X.-Q. Zhao, W. Shi and Y. Song, *Inorg. Chem.*, 2009, **48**, 3493; (d) L. F. Marquesa, C. C. Corrêaa, R. Rosa da Silvab, M. Vieira dos Santosb, S. J. L. Ribeirob and F. C. Machado, *Inorg. Chem. Commun.*, 2013, **37**, 66; (e) Y.-G. Sun, B. Jiang, T.-F. Cui, G. Xiong, P. F. Smet, F. Ding, E.-J. Gao, T.-Y. Lv, K. Van den Eeckhout, D. Poelman and F. Verpoort, *Dalton Trans.*, 2011, **40**, 11581; (f) J. Zhang, J. T. Bu, S. Chen, T. Wu, S. Zheng, Y. Chen, R. A. Nieto, P. Feng and X. Bu, *Angew. Chem. Int. Ed.*, 2010, **49**, 8876; (g) W. Huang, D. Wu, P. Zhou, W. Yan, D. Guo, C. Duan and Q. Meng, *Cryst. Growth Des.*, 2009, **9**, 1361; (h) M.-X. Wang, L.-S. Long, R.-B. Huang and L.-S. Zheng, *Chem. Commun.*, 2011, **47**, 9834; (i) C.-H. Zhan, F. Wang, Y. Kang and J. Zhang, *Inorg. Chem.*, 2012, **51**, 523; (j) Z.-H. Li, T. Zhang, L.-P. Xue, S.-B. Miao, B.-T. Zhao, J. Kan and W.-P. Su, *CrystEngComm*, 2013, **15**, 7423.
- 8 L.-P. Xue, X.-H. Chang, S.-H. Li, L.-F. Ma and L.-Y. Wang, *Dalton Trans.*, 2014, **43**, 7219.
- 9 Y.-H. Chao, S.-C. Kuo, K. Ku, I.-P. Chiu, C.-H. Wu, A. Mauger, H.-K. Wang and K.-H. Lee, *Bioorg. Med. Chem.*, 1999, **7**, 1025.
- 10 G. M. Sheldrick, *SADABS, Program for Siemens Area Detector Absorption Corrections*, University of Göttingen, Germany, 1997.
- 11 (a) G.M. Sheldrick, SHELXTL Version 5.1. Bruker Analytical X-ray Instruments Inc., Madison, Wisconsin, USA, 1998; (b) G. M. Sheldrick, SHELXL-97, *Program for the Refinement of Crystal Structure*; University of Göttingen, Germany, 1997.
- 12 (a) H. S. Huh and S. W. Lee, *Bull. Korean Chem. Soc.*, 2006, **27**, 1839; (b) A.-H. Yang, J.-Y. Zou, W.-M. Wang, X.-Y. Shi, H.-L. Gao, J.-Z. Cui and B. Zhao, *Inorg. Chem.*, 2014, **53**, 7092.
- 13 (a) E. Neofotistou, C. D. Malliakas and P. N. Trikalitis, *CrystEngComm*, 2010, **12**, 1034; (b) J.-D. Lin, S.-T. Wu, Z.-H. Li and S.-W. Du, *Dalton Trans.*, 2010, **39**, 10719; (c) L. Yan, Q. Yue, Q.-X. Jia, G. Lemerrier and E.-Q. Gao, *Cryst. Growth Des.*, 2009, **9**, 2984; (d) I. A. Baburin and V. A. Blatov, *Acta Cryst.*, 2007, **B63**, 791.
- 14 (a) B. R. Judd, *Phys. Rev.*, 1962, **127**, 750; (b) G. S. Ofelt, *J. Chem. Phys.*, 1962, **37**, 511.
- 15 M. Gustafsson, A. Bartoszewicz, B. Martín-Matute, J. Sun, J. Grins, T. Zhao, Z. Li, G. Zhu and X. Zou, *Chem. Mater.*, 2010, **22**, 3316.